2011

Fluorinated Templates for Energy-Related Nanomaterials and Applications

Mohammed J. Meziani
Clemson University

Fushen Lu
Clemson University

Li Cao
Clemson University

Christopher E. Bunker
Air Force Research Laboratory

Elena A. Guliants
University of Dayton, eguliants1@udayton.edu

See next page for additional authors

Chapter 7

Fluorinated Templates for Energy-Related Nanomaterials and Applications

Mohammed J. Meziani,*,† Fushen Lu,† Li Cao,† Christopher E. Bunker,*,‡ Elena A. Guliants,¶ and Ya-Ping Sun*,†

†Department of Chemistry and Laboratory for Emerging Materials and Technology, Clemson University, Clemson, South Carolina 29634-0973
‡Air Force Research Laboratory, Propulsion Directorate, Wright-Patterson Air Force Base, Ohio 45433-7103
¶University of Dayton Research Institute, Sensors Technology Office, Dayton, Ohio 45469
***Corresponding authors: mmezian@clemson.edu, christopher.bunker@wpafb.af.mil, and syaping@clemson.edu**

Fluorinated ionomer membranes, as represented by the commercially available Nafion films, are macroscopically homogeneous and optically transparent but microscopically inhomogeneous with the presence of nanoscale hydrophilic cavities. These cavities serve as nanoscale reactors for the synthesis of nanoparticles from a variety of materials. The membranes with embedded nanoscale semiconductors, still optically transparent, have been used as sheet-photocatalysts for energy conversion applications, while those with embedded reactive metals used as nano-energetic materials for hydrogen generation and beyond. This chapter provides an overview on the templated synthesis of nanomaterials in fluorinated ionomer membranes and the various energy-related applications of this unique class of nanocomposite materials.

1. Introduction

The combination of fluorinated entities and nanoscale materials has received much recent attention for existing and emerging opportunities in a variety of energy-related applications, such as energy saving (*1*), optoelectronic (lighting)

(*2*), catalysis (*3–8*), nanothermite reactions (*9*, *10*), and hydrogen fuel sources (*11*, *12*). Fluorine-containing materials are unique in many desirable properties due to the highest electronegativity and small atomic radius of fluorine. These distinctive properties include high thermal and chemical stability, solvent resistance, low flammability, low moisture absorption, low surface tension/energy, low dielectric constant, and strong oxidant source under energetic conditions (*3*). Among the best-known and most widely used fluorine-containing materials are organic and polymeric compounds with fluorine functional groups (*3*, *10–28*), particularly fluorinated surfactants such as high-molecular weight perfluorinated acids (*3*, *10*, *11*, *13*) and perfluorinated ionomer membranes, with the latter being represented by the commercially available Nafion membrane films (*12*, *14–28*).

Nafion (Scheme 1) is a perfluorinated sulfonic acid polymer with excellent thermal, chemical and mechanical stability and high ionic conductivity (*14*, *16*). Because of these characteristics, Nafion membrane has been the membrane of choice for applications in aggressive chemical environments, such as separators in chloro-alkali cells (*15*, *16*), modern battery and fuel cell technologies (*14–16*), sensors (*15*), and super-acid catalysis for the production of fine chemicals (*17*). For example, Nafion was found to be effective as a membrane for hydrogen/oxygen and direct methanol proton exchange membrane (PEM) fuel cells by permitting hydrogen ion transport while preventing electron conduction, thus providing unparalleled power supply from hydrogen (*14–16*). The Nafion properties are further expanded through its ability to preconcentrate cationic species, making it possible to host a wide range of entities such as redox mediators (*18*) and nanoparticles (*5–8*, *12*, *19–23*) for more efficient catalytic and energetic applications (*5–8*, *12*, *29*). Some of the most exciting developments have been their coupling with nanoscale semiconductor and reactive powders for the photoreduction of CO_2 and evolution of hydrogen (*5–8*, *12*). For example, Nafion membrane was found recently to be an ideal template for the preparation of small and air-stable Al nanoparticles with potential energetic applications (*12*).

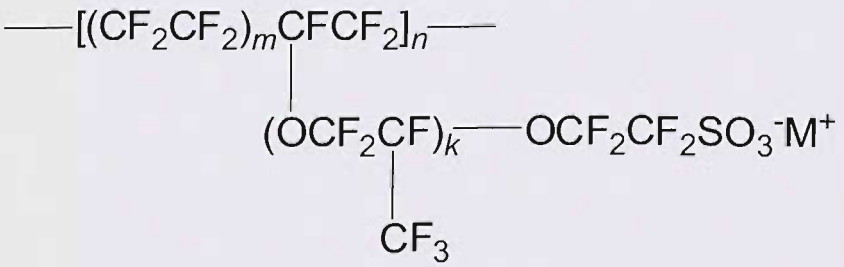

Scheme 1. Nafion.

In this chapter, we first provide some background information on and the current understanding of the structure and properties of perfluorinated ionomer membranes, and then highlight recent developments in the use of these membranes for the synthesis of small and size-wise narrowly distributed semiconductor and metal nanoparticles and their selected energy-related applications. We conclude with a brief summary of the challenges and perspectives in this interdisciplinary research field.

2. Fluorinated Ionomer Membranes

Perfluorinated membranes generally refer to ion-exchange membranes with a perfluorinated polymer backbone. These membranes typically exhibit excellent thermal and chemical stability with retention of mechanical properties in highly corrosive and oxidative environments. A representative example is the Nafion membrane (*14–17*), in which the underlying polymer is a sulfonated tetrafluoroethylene-based fluoropolymer-copolymer (Scheme 1). The synthesis of Nafion polymer is achieved via the copolymerization of tetrafluoroethylene (TFE) (the monomer in the widely used Teflon) and a derivative of perfluoro(alkyl vinyl ether) with sulfonyl acid fluoride, followed by the conversion of sulfonyl fluoride into sulfonate groups and then into the acid form. Finally, the polymer solution is cast into thin films via heating in aqueous alcohol at 250 °C in an autoclave (*15*).

The pendant ionic groups interact to form ion-rich aggregates contained in a nonpolar matrix, which strongly influences the polymer properties and applications. Although Nafion polymers in the membrane are not covalently crosslinked, the membrane structure is highly ordered. Microscopically, the structure and properties of perfluorinated ionomer membranes have been understood in terms of a reverse micelle-like ion cluster model developed in the study of Nafion (*4*, *15*, *24*, *25*). According to the model there are essentially three distinctive structural regions in the membrane: the perfluorinated polymer network, hydrophilic cores or ion clusters, and the interfacial domain between the two regions (Scheme 2). The hydrophilic cores or ion clusters are estimated as being on the order of 4 nm in diameter, in part based on experimental results primarily from small-angle X-ray studies (*24*, *25*). The neighboring clusters are interconnected through narrow channels (Scheme 2) (*15*, *25*). While there is some experimental evidence in support of such a structural model, issues including the shape and morphology of the ion clusters, the significance and dimension of the interfacial region, and the general organization of hydrophilic and hydrophobic structural domains in Nafion and related ionomer membranes are still being debated and investigated (*26*, *27*). For example, luminescence spectroscopic methods have been employed to study the structural properties of ionomer membranes, including an evaluation of the ion cluster model illustrated in Scheme 2 (*26–28*). Results from the use of a series of environment-sensitive fluorescent probes such as $Ru(bpy)_3^{2+}$, pyrene with excimer formation, and ethidium bromide have suggested the presence of a substantial interfacial region in perfluorinated ionomer membranes (*26–28*). It was proposed that the interfacial region could be viewed as a heterogeneous mixture of perfluorinated polymer branches and water

molecules, where the microscopic environment experienced by the fluorescent molecular probes might effectively be close to those in polar organic solvents (*27*). Results from the luminescence spectroscopic studies have also provided valuable information on the transport-related processes in the ionomer membrane, suggesting considerable mobility throughout the interfacial region, as reflected by the significant diffusional fluorescence quenching for probes in the membrane structural domain (*27*).

The microscopic structure in the ionomer membranes, as described by the ion cluster model (Scheme 2), has major implications to the primary uses of these membranes, such as in fuel cells (*14–16*). Equally significant is the fact that these membrane films are macroscopically homogeneous, uniform and optically highly transparent, but microscopically heterogeneous with hydrophilic ion clusters dispersed in fluorinated polymer backbones, thus offering an excellent platform for templated synthesis of nanoscale materials.

3. Nano-Templating for Energy-Related Applications

The presence of hydrophilic cavities in the ionomer Nafion membrane structure was also supported by experiments in which nanoparticles were prepared by using the cavities in Nafion membrane as templates (*5–8*, *12*, *19–23*). In fact, the incorporation of nanoparticles into the membrane served another purpose by allowing a direct imaging of the hosting cavities in the membrane structure, complementary to the electron microscopy studies of stained Nafion membrane films. For example, Sun and coworkers reported the preparation and characterization of several crystalline semiconductor and metal nanoparticles including PbS, CdS, Ag_2S, and Ag in various perfuorinated ionomer membranes including Nafion and those based on the sulfonimide ionomer and the bis(sulfonyl)methane ionomer (*20*, *21*, *23*). Overall, the nanoparticles were easy to prepare and air-stable, and could easily be handled under ambient conditions.

Experimentally for the preparation of Ag_2S nanoparticles as an example (*20*), a piece of clean Nafion film in the sodium form was soaked in an aqueous solution of $AgNO_3$, followed by rinsing with water to clean the film surface. After the surface was blotted dry, the film containing Ag^+ was immersed in an aqueous solution of Na_2S for the formation of Ag_2S particles under fully hydrated condition. The same procedure and similar experimental parameters were used in the preparation of semiconductor nanoparticles. These nanoparticles could be identified by using UV/vis absorption and luminescence, X-ray powder diffraction (XRD), and transmission electron microscopy (TEM, specimen from cross-sectional slices of the Nafion film loaded with nanoparticles) methods. Examples for the results from characterizations are shown in Figure 1 (*20*, *21*). These nanoparticles were apparently mostly crystalline, small in sizes and with narrow size distributions (*20*, *21*). Microscopically, the nanoparticles were found as being hosted in the membrane structure in an isolated fashion, with no indication of channels-like domains as proposed in the ion cluster model for the ionomer membranes. The results suggested that all of these membrane films contain hydrophilic structural cavities and likely share similar nanoscopic

structures. However, the randomly dispersed Ag_2S nanoparticles were found to be significantly larger than the average size of the reverse micelle-like hydrophilic cavities predicted and/or estimated in the literature for Nafion membrane. A possible explanation for the discrepancy could be that the membrane structure with the ion clusters is somewhat flexible, thus to allow the extra growth of particles (for some materials such as Ag_2S) in the hydrophilic cavities via squeezing the connecting channels.

The nanoscale Ag particles in the structural cavities of Nafion membrane were prepared under similar experimental conditions as those used for Ag_2S, except that $NaBH_4$ was used instead of Na_2S (*23*). The UV/vis absorption spectrum of the membrane post-reaction exhibited the characteristic surface plasmon absorption band of nanoscale Ag (Figure 2). XRD and TEM analyses confirmed the formation of well-dispersed face-centered-cubic crystalline Ag nanoparticles (an average size of 13.4 nm in diameter and a size distribution standard deviation of 2.2 nm, Figure 2). The sizes were comparable to those of the Ag_2S nanoparticles discussed above, again obviously much larger than the predicted and/or estimated average cavity size in the Nafion membrane according to the ion cluster model. The results were also explained such that the hydrophilic cavities and channels must be structurally flexible enough to accommodate the formation of the larger Ag nanoparticles (*23*). More interestingly, the population of Ag nanoparticles in the membrane structure was found to vary with changes in the concentraton of the aqueous $AgNO_3$ solution (Figure 3), but the sizes of these nanoparticles remained generally similar. In fact, the film samples prepared with loading at higher $AgNO_3$ concentrations contained larger populations of Ag nanoparticles (Figure 3) (*23*). The variation of nanoparticle contents in the films was made evident by the UV/vis absorption, XRD, and TEM results. As compared in Figure 3, the characteristic plasmon absorption band obviously increases with the $AgNO_3$ solution concentration used in soaking the film in the nanoparticle preparation. The lower loading of Ag nanoparticles is also obvious in the TEM image shown in Figure 3, in comparison with the image in Figure 2 for the film corresponding to a much more concentrated $AgNO_3$ solution. However, despite the smaller number, the sizes of the Ag nanoparticles remain to be around 13 nm, rather similar to those shown in Figure 2.

These examples discussed above demonstrate that nanoscale semiconductor and metal nanoparticles can be embedded in fluorinated ionomer membranes, specifically in Nafion, to result in composite films. These essentially nanocomposites are generally stable (obviously free from any agglomeration), amenable to a variety of energy-related applications. As highlighted below, their uses as sheet-photocatalysts in energy conversion and as nano-energetic materials are particularly interesting (*5–8*, *12*).

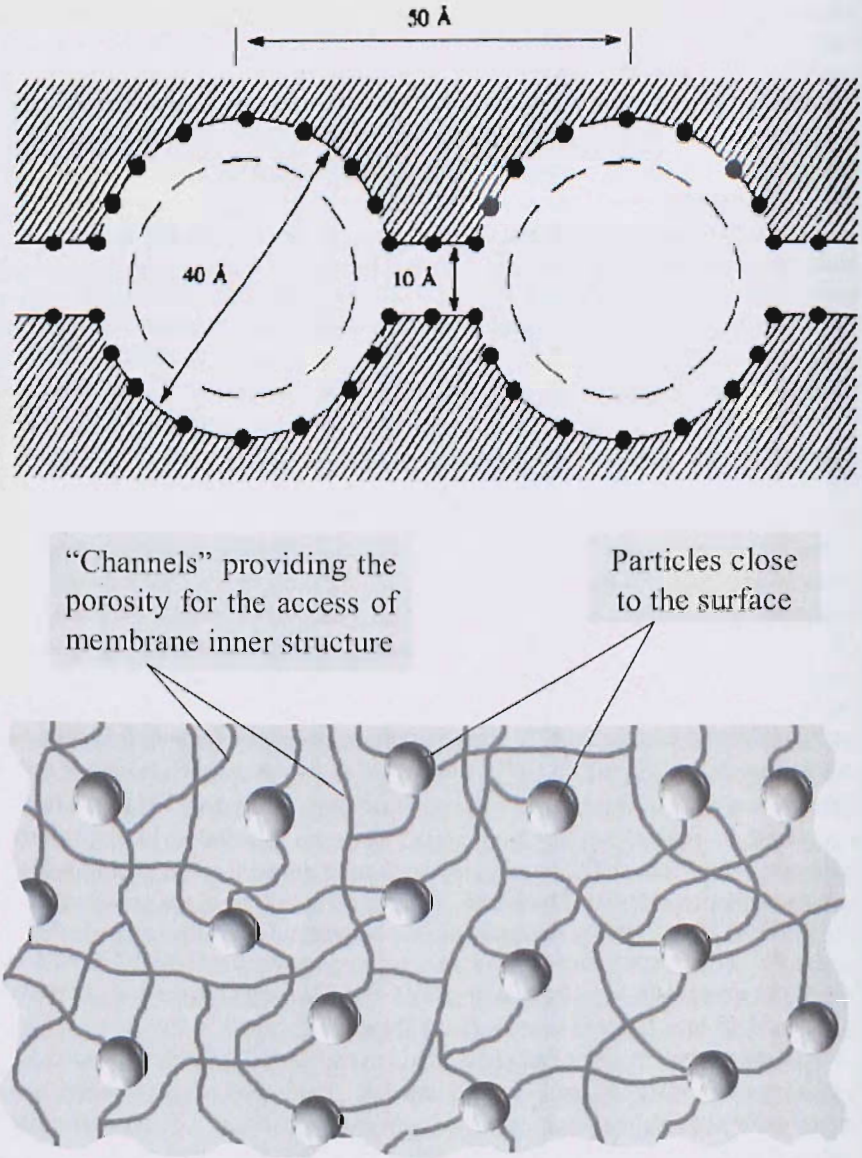

Scheme 2. Cartoon illustrations for the proposed structure of ion clusters for perfluorinated ionomer membranes (top) (From ref. (15, 24)) and a cross-sectional view of the Nafion membrane film embedded with nanoparticles (bottom).

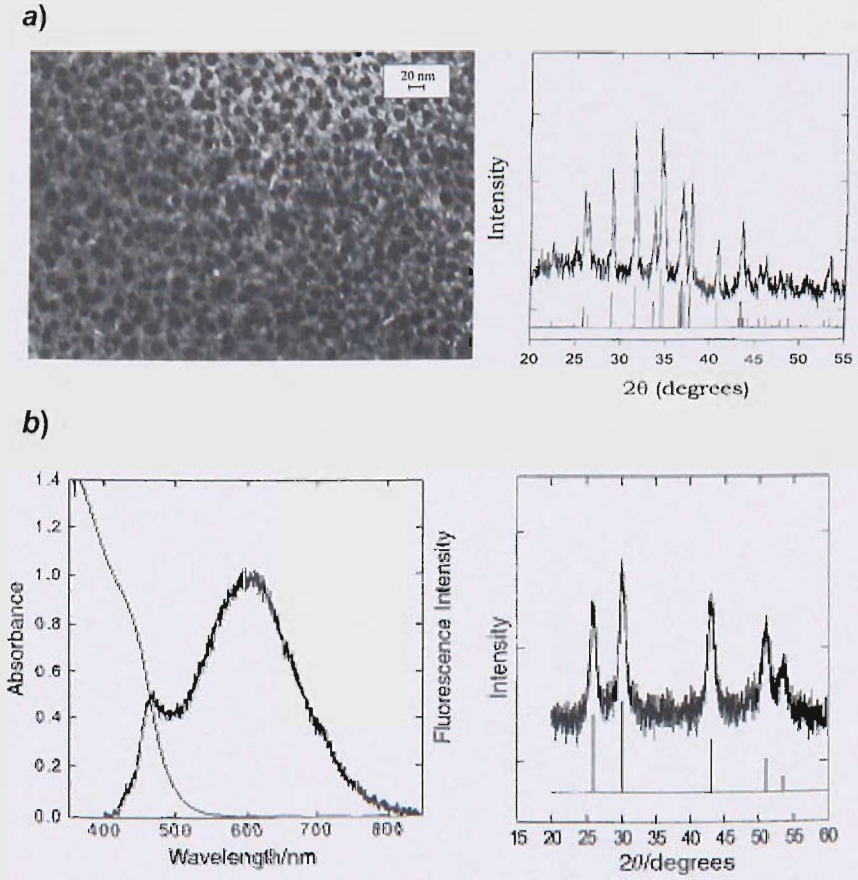

Figure 1. (a) TEM image for a cross-sectional view (left) and X-ray diffraction pattern (right) of Ag_2S nanoparticles embedded in structural cavities of Nafion membrane. (From ref. (20)) (b) Absorption and fluorescence spectra of CdS nanoparticles (left) and the X-ray diffraction pattern of PbS nanoparticles (right) embedded in structural cavities of Nafion membrane. (From ref. (21)).

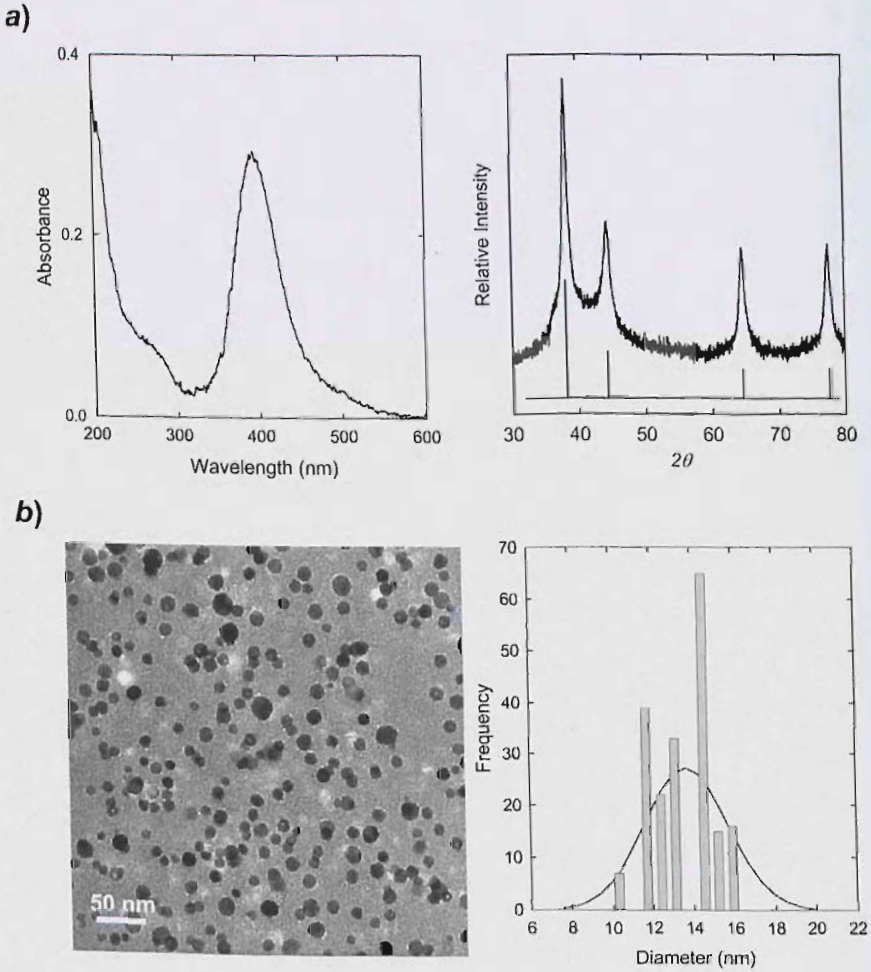

Figure 2. (a) The UV/vis absorption spectrum (left) and the X-ray diffraction pattern (right), and (b) TEM image for a cross-sectional view (left) and a statistical size analysis (right) of silver nanoparticles in Nafion membrane prepared with a more concentrated $AgNO_3$ solution. (From ref. (23)).

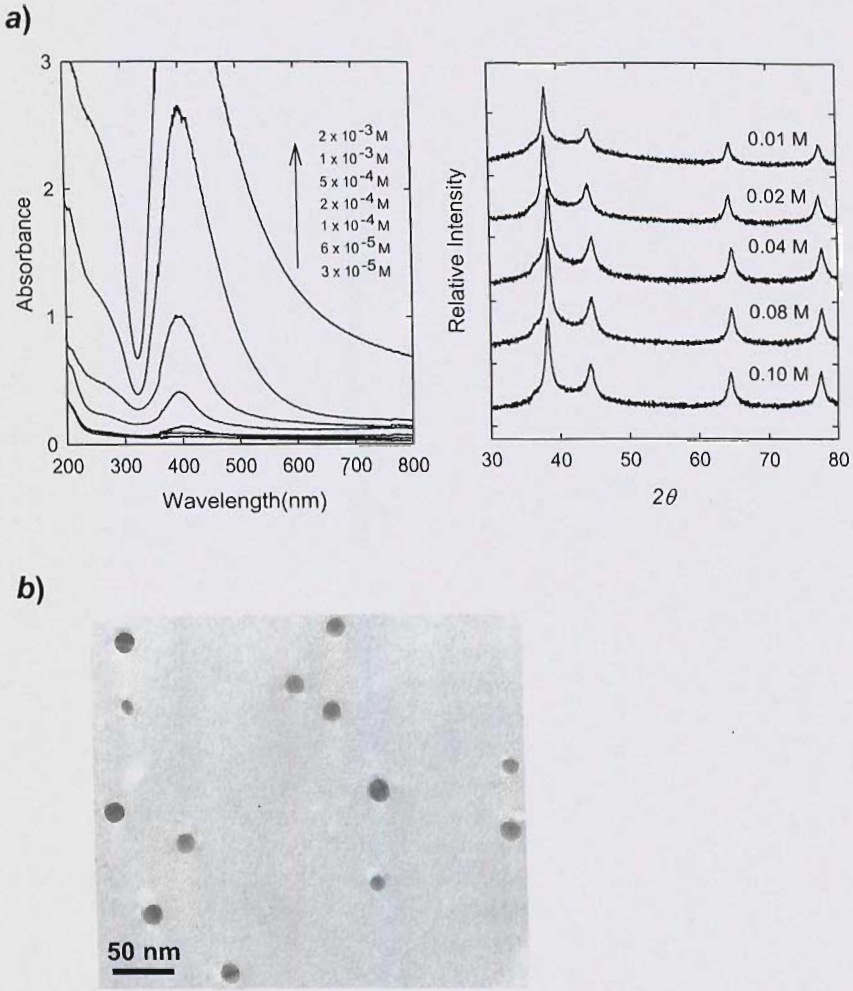

Figure 3. (a) UV/vis absorption spectra (left) and powder X-ray diffraction patterns (right) of silver nanoparticles in Nafion membrane films corresponding to soaking the films in aqueous $AgNO_3$ solutions of different concentrations (as marked) for a constant 30 min. (b) TEM image for a cross-sectional view of silver nanoparticles in the Nafion membrane film corresponding to soaking the film in aqueous $AgNO_3$ solution of 1 mM for 30 min. (From ref. (23)).

3.1. Sheet-Photocatalysts for Energy Conversion

The Nafion films loaded with nanoscale semiconductor particles could remain optically transparent when the nanoparticle population is appropriately controlled. These are effectively semiconductor-based sheet-photocatalysts (*5–8*). The optical transparency of the nanocomposite films as photocatalysts has made it possible to more effectively utilize the incident light and maximize the nanoparticle surface area for high photocatalytic activities (*5–8*). For example, nanoscale semiconductors CdS and TiO_2 and their nanocomposites such as CdS/ZnS and CdS/Pt were prepared in Nafion membrane for evaluations in the photocatalytic production of hydrogen (*5*). In the reported studies, the hydrogen-production efficiencies from water containing a sacrificial electron donor (sulfide ion) were found to be greater than those commonly obtained with unsupported colloidal or powdered semiconductors under similar conditions .

Sun and coworkers studied the photoreduction of CO_2 by using TiO_2 nanoparticles without and with the coated Ag as a co-catalyst embedded in Nafion membrane films (*7*, *8*). For the preparation of TiO_2 and Ag/TiO_2 in nanoscale cavities of Nafion membrane (*7*, *8*, *22*), a clean Nafion film was first soaked in a solution of $Ti(OC_3H_7)_4$ in isopropanol, washed with isopropanol and acetone, and then immersed in boiling water for hydrolysis to form the targeted TiO_2 nanoparticles. The TiO_2-loaded Nafion films appeared similar to the starting blank films, except for a light yellowish color (due to the absorption of the embedded nanoparticles). The TiO_2 nanoparticles embedded in Nafion membrane films were then coated with Ag metal via photolysis (*8*). The resulting film was brownish, consistent with the presence of nanoscale Ag (plasmon absorption), but remained optically transparent. The amount of Ag deposition was found to depend on the concentration of the $AgNO_3$ solution used in the coating. UV/vis absorption and TEM (specimen from cross-sectional microtome) analyses of TiO_2-loaded films without and with the Ag coating are shown in Figure 4. The embedded nanoparticles appeared crystalline and well-dispersed. The nanoparticles became somewhat larger after the Ag coating, 6.5 nm vs 4 nm (Figure 4). The association of Ag with TiO_2 at the nanoscale was also confirmed by the energy dispersive X-ray (EDX) analysis of randomly selected regions in the image, all of which indicated the substantial presence of Ti together with Ag.

The sheet-photocatalysts were evaluated for the photoreduction of liquid CO_2. The configuration of the catalyst films in the high-pressure optical cell of the reaction setup is illustrated in Scheme 3. In a typical experiment, the cell was purged with CO_2 gas for 30 min before it was filled with liquid CO_2 to a pressure of 2,000 psia, followed by photoirradiation with a xenon arc source. Post photoirradiation, the cell was depressurized and water was added to the cell immediately thereafter (*7*, *8*). The resulting aqueous solution contained methanol, acetic acid, and formic acid as the reaction products according to HPLC and ^1H NMR analyses (*7*, *8*). As shown in Figure 5, the results suggest that these sheet-photocatalysts are effective in improving the photocatalytic conversion of CO_2 (in comparison with results from other experimental configurations). The Ag coating apparently enhanced the photoconversion. These sheet-photocatalysts

were also found to be highly stable chemically and photochemically, reusable in repeated photocatalytic reactions (*7*, *8*).

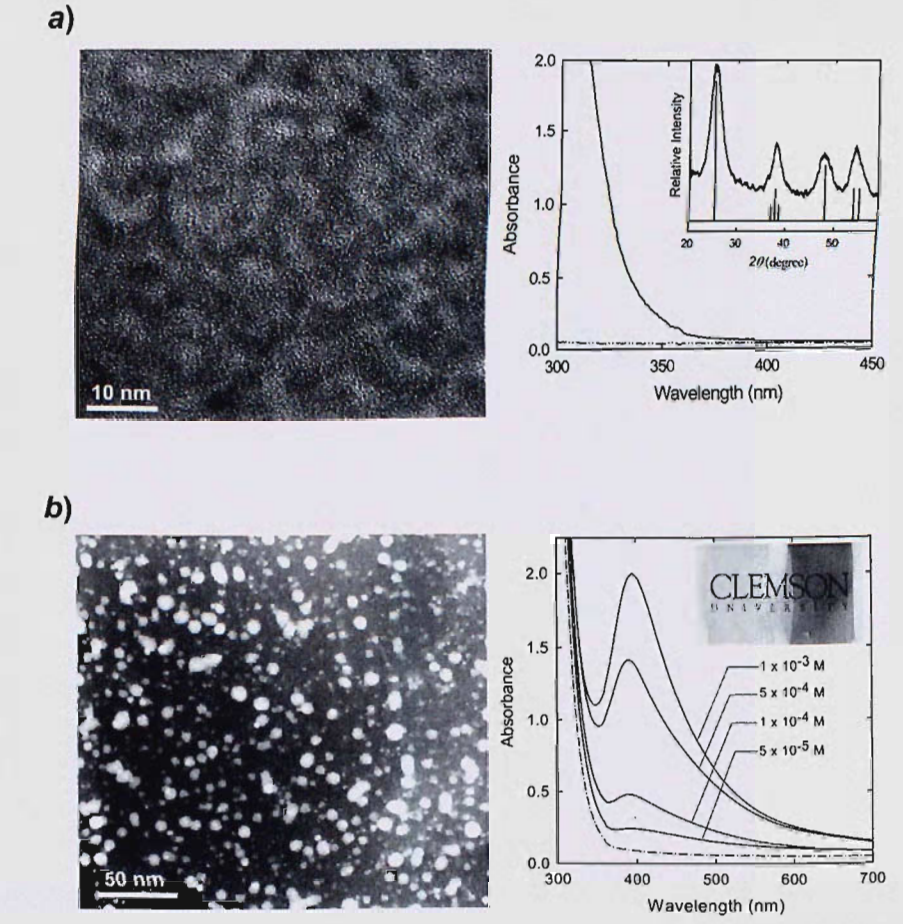

Figure 4. (a) High-resolution TEM image for a cross-sectional view of the TiO_2 nanoparticles in Nafion membrane (left), and UV/vis absorption spectra of Nafion films with (——) and without (— · —) embedded TiO_2 nanoparticles, with the inset showing the powder X-ray diffraction pattern of the TiO_2-loaded Nafion film (right). (From ref. (7) and (22)) (b) Scanning TEM image (in the Z-contrast mode) for a cross-sectional view of the silver-coated TiO_2 nanoparticles in Nafion membrane films (left), and UV/vis absorption spectra of Nafion membrane films containing TiO_2 nanoparticles without (— · —) and with (——) the silver coating (the corresponding silver salt solution concentrations used for the coating as marked), and the inset: photos of the corresponding films (right). (From ref. (8)).

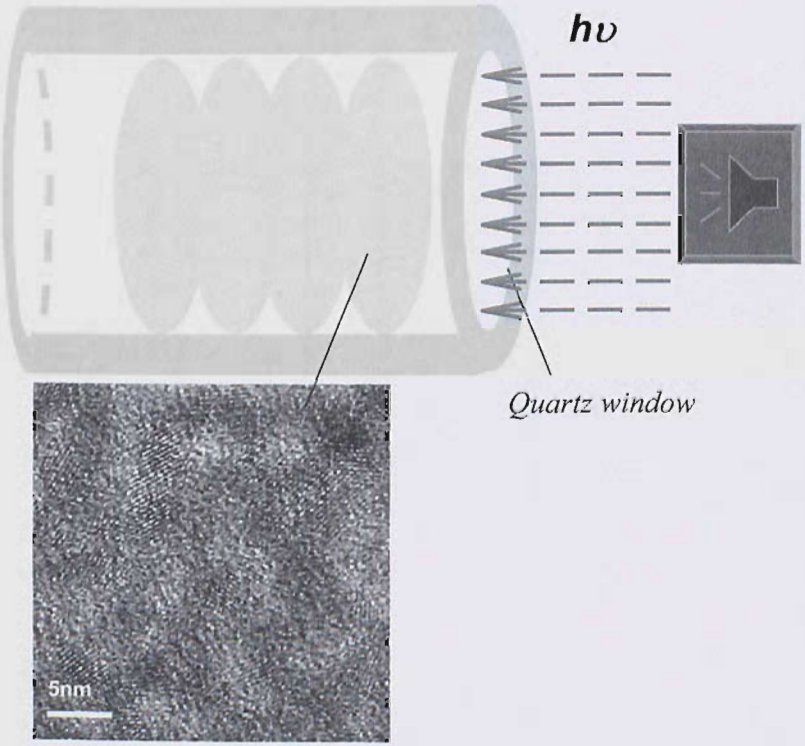

Scheme 3. Experimental setup for the photoreduction of liquid CO_2 with TiO_2-loaded Nafion films as photocatalyst. The TEM image is for a specimen from the cross-sectional microtome of a TiO_2-loaded film. (From ref. (7)).

The facile synthesis of semiconductor nanoparticles in Nafion membrane and the subsequent coating of the nanoparticles with a co-catalyst should be generally applicable to the preparation of other conceptually similar sheet-photocatalysts. In such a configuration, the membrane serves as an optically transparent host for the homogeneous dispersion of the catalytic nanoparticles. These photocatalysts in a uniquely well-dispersed configuration are valuable to various energy conversion applications.

3.2. Energetic Nanoparticles

The characteristic structure and properties of perfluorinated ionomer membranes discussed above and their ability to encapsulate and protect nanoparticles have also made them uniquely applicable in the development of nano-energetic materials. Nanosized (sub-100 nm) Al particles have recently been among the most widely investigated reactive and energetic nanomaterials (*10*, *11*, *30–33*). Their large specific surface area and energy density, when coupled

or mixed with oxidative species, make them unique combustible additives in propellant formulations, among other fuel-related applications (*34*). Nanoscale Al particles are also studied as high-capacity hydrogen storage materials (*35*). Significant effort has been made on the development of synthetic methodologies for Al nanoparticles of desired properties (*10*, *11*, *30–33*, *36*). The chemical route based on thermal and/or catalytic decomposition of alane in the presence of a surface passivation agent such as perfluorinated carboxylic acids for particle protection and stabilization has been identified as being particularly promising (*10*, *11*). However, this method has generally yielded Al particles of 50 – 200 nm in average sizes. Smaller Al nanoparticles (thus an extremely high surface area) of a narrow size distribution have been pursued for their distinctive advantageous in uses as energetic nanomaterials and for more effective hydrogen generation. However, their bulk production in a consistent fashion and their protection for stability under ambient conditions present special challenges.

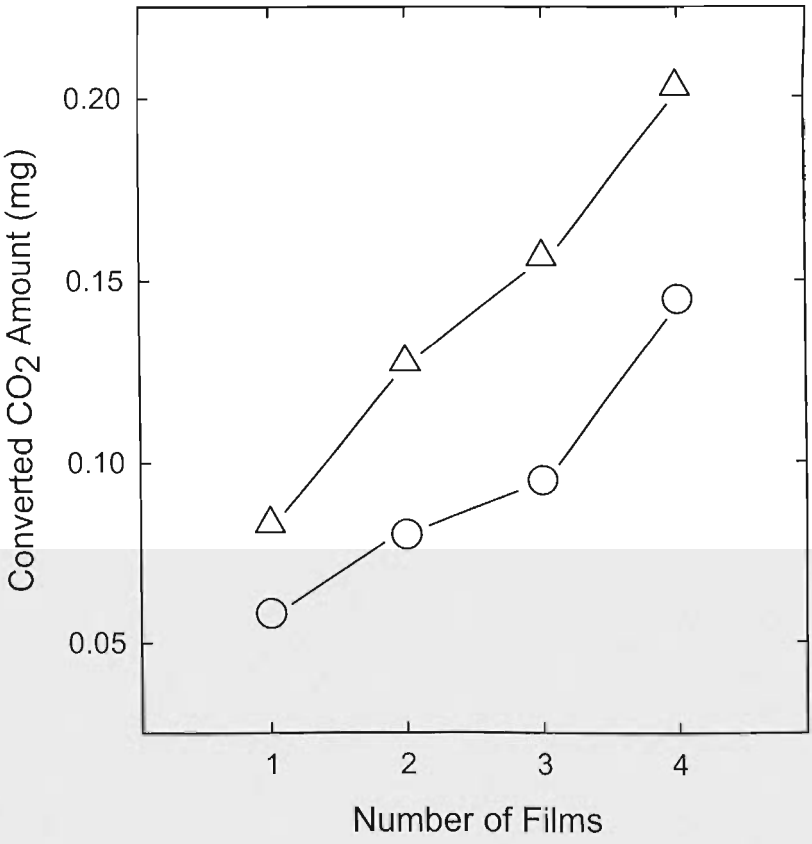

Figure 5. The photoconversion of CO_2 as a function of the number of stacked catalytic films with (Δ) and without (o) the silver coating of the embedded TiO_2 nanoparticles. The reproducibility for the data points was generally within ~3%. (From ref. (8)).

Sun and coworkers reported recently a new strategy in the facile yet controllable synthesis of smaller Al nanoparticles by using nanoscale cavities in Nafion membrane as templates. The nano-templated synthesis was based on the same catalytic alane decomposition chemistry. Experimentally, a piece of Nafion film in the sodium form was soaked in an isopropanol solution of $Ti(OC_3H_7)_4$, rinsed thoroughly to clean the film surface, and then dried. The Nafion film containing the titanium salt was immersed in a THF solution of 1-methylpyrrolidine alane with stirring in a glove-box under nitrogen atmosphere. The film color turned black during the reaction, consistent with the formation of small Al nanoparticles. After the reaction the film was thoroughly washed with THF, dried under vacuum, and then characterized by using a series of techniques. Shown in Figure 6 are low and high resolution TEM images (with the specimen from cross-sectional microtome), a statistical size analysis of particles from multiple TEM images, and also representative results from the EDX analysis (*12*). The randomly dispersed Al nanoparticles appeared crystalline (agreeing well with the face-centered-cubic standard for bulk Al (Figure 6), with an average particle size of 11 nm in diameter and a size distribution standard deviation of 2.5 nm. The EDX results confirmed the presence of large amounts of Al and fluorine (a part of the Nafion membrane structure) and a small amount of titanium from the catalyst. However, there was only a negligible amount of oxygen in the specimen despite the fact that the EDX analysis was performed under ambient conditions, suggesting that the embedded Al nanoparticles were protected by the membrane structure from any significant oxidation (*12*).

More detailed studies on the formation of Al nanoparticles in Nafion membrane suggested that significant variations in the amount of embedded materials in the membrane changed primarily the population of the nanoparticles, but affected much less the sizes of the particles, as suggested by the XRD results (Figure 7) (*12*). The results and conclusion were rather similar to those obtained previously in the systematic study of Ag nanoparticles in perfluorinated ionomer membranes (*23*). The population of Al nanoparticles in the Nafion membrane was increased by using a more concentrated alane solution in the reaction. With the use of high alane concentrations in the particle synthesis, the Nafion membrane films were apparently able to host a substantial amount of Al nanoparticles, as demonstrated by the obvious weight increases of the films post-alane reaction (Figure 8). For example, with alane solutions of 0.5 M and 2 M used in the reaction, the resulting films had weight increases of 14% and 122% (thus the implied Al contents in the films of 12% and 55%), respectively. Both the thermogravimetric analysis (TGA) and hydrogen generation results suggested that the weight increase was due to the amount of reactive Al in the film. For the latter, it was found that the reactive Al contents in the films could be determined accurately by using the films to generate hydrogen gas in a basic aqueous solution (*37*). The experiments were performed in a commercially supplied apparatus to allow precise volumetric measurements of the hydrogen gas generated for the calculation of the reactive Al contents. For the same example, the amounts of Al nanoparticles in the films prepared with 0.5 M and 2 M alane solutions were determined to be 11% and 57% of the film weights, in good agreement with the observed weight increases post-alane reaction discussed above. Results from the

XRD analysis and TEM imaging of the cross-sectional slices of the Al-in-Nafion composite films with high Al loadings suggested that the films were packed with Al nanoparticles, while the particle sizes remained generally similar, suggesting again that the different loadings of Al nanoparticles in the Nafion membrane films are generally decoupled from the average sizes of the nanoparticles.

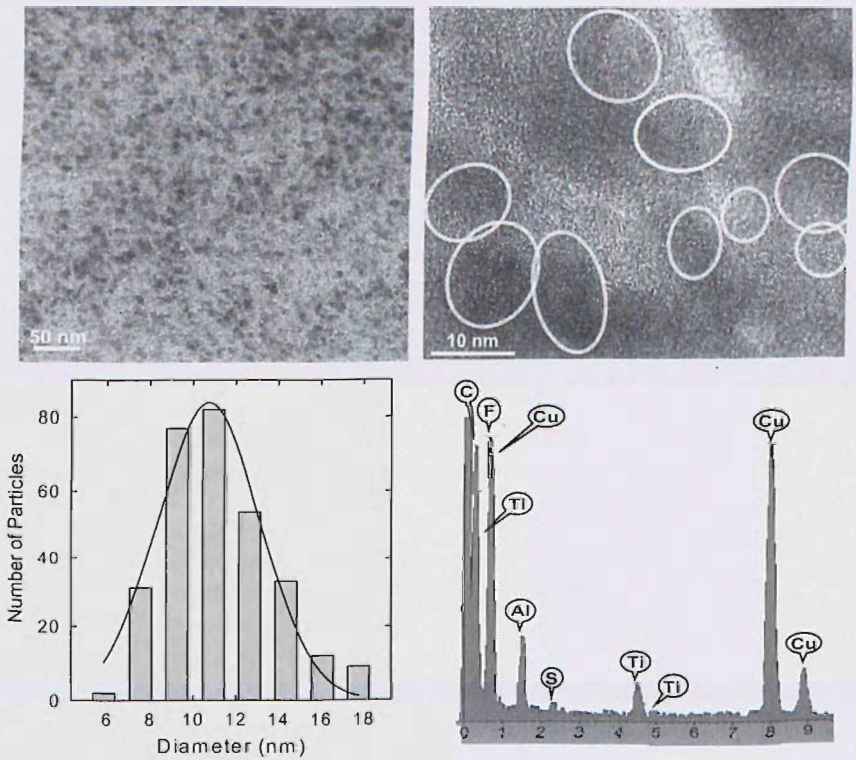

Figure 6. A representative TEM image for the specimen from ultra-microtome of an Al-in-Nafion film (top left), a statistical size analysis of the particles from multiple images (bottom left), and the corresponding high-resolution TEM image for the specimen from ultra-microtome (top right) and the EDX spectrum (bottom right). (From ref. (12)).

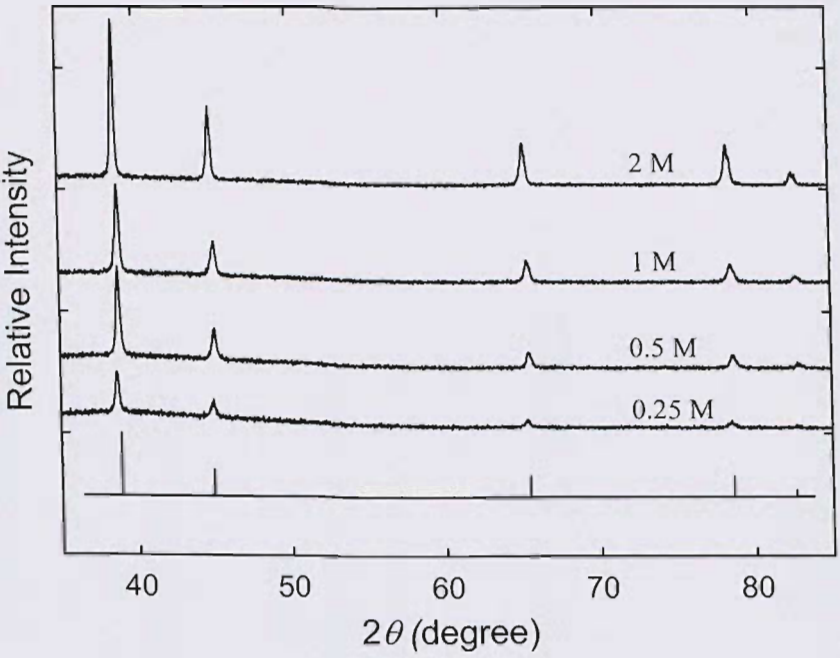

Figure 7. X-ray diffraction patterns of the Al-in-Nafion films prepared with different alane solution concentrations (as marked) are compared with that of bulk fcc aluminum in JCPDS database.

As reported (*12*), all of the Al-in-Nafion film samples were found to be surprisingly stable in ambient air, with the reactive Al contents changed only marginally over time (Figure 9). The relatively more significant initial decrease in the reactive Al content might be attributed to the oxidation of the Al nanoparticles close to the film surface. The small sacrifice of these nanoparticles due to the oxidation probably "sealed off" the composite film as a whole, minimizing any subsequent oxidation. The Nafion membrane structure was apparently not permeable to oxygen under the ambient air conditions, preventing any substantial oxidation of the embedded Al nanoparticles. On the other hand, the Al nanoparticles were fully accessible under the hydrolysis conditions for the nearly quantitative generation of hydrogen gas. Therefore, the Al-in-Nafion composite films may serve as a unique platform for stable energetic materials and/or as materials for energy storage.

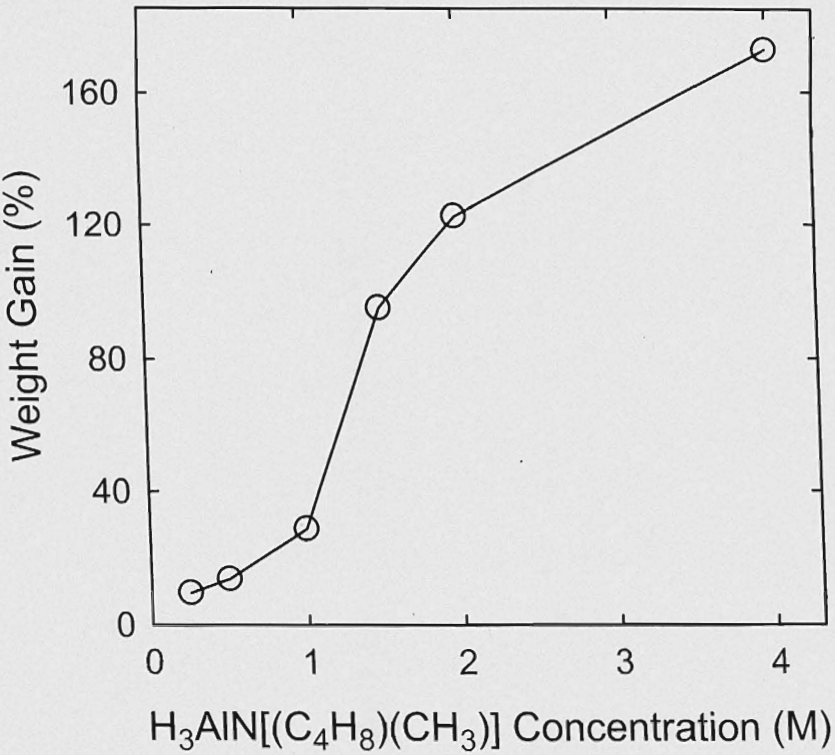

Figure 8. The weight increase in the composites of Al nanoparticles in Nafion membrane as a function of the alane concentration in the reaction for the preparation of these composite films.

The Nafion membrane films embedded with Al nanoparticles, especially those with high loadings, were found to be easily crushed via grinding in a mortar to form black-gray powdery materials. These materials were subsequently dispersed in solvents such as hexane with sonication, though the resulting suspension was unstable (with significant precipitation within a few minutes). Interestingly, however, the Al nanoparticles were largely unaffected in the process, maintaining their sizes and dispersion according to electron microscopy (Figure 10) and XRD results. These powders were essentially Al nanoparticles protected and stabilized by Nafion polymers (disintegrated backbones in the original membrane film).

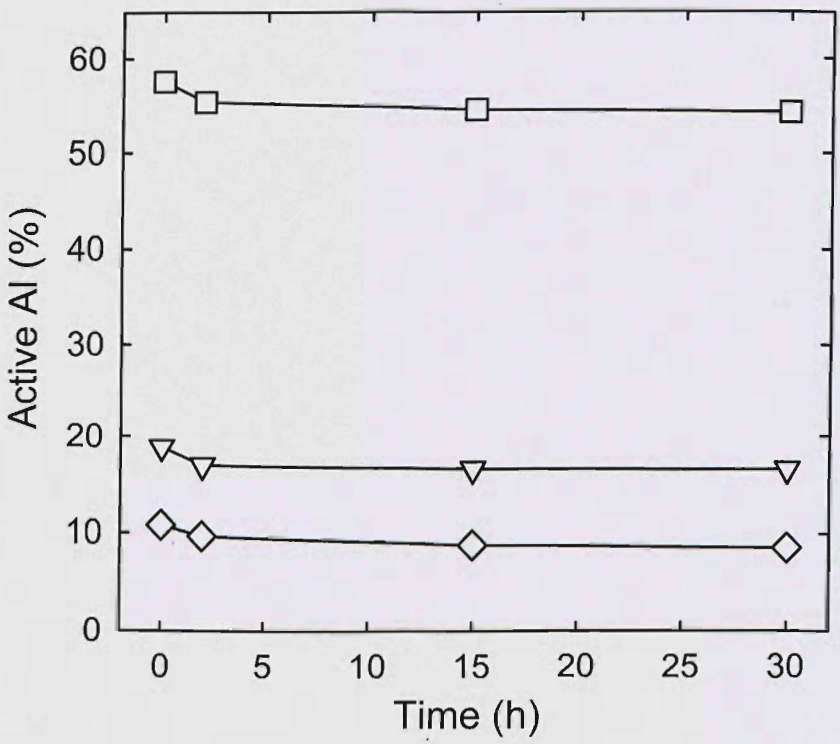

Figure 9. The reactive Al contents in the various Al-in-Nafion films (based on volumetric measurements of the hydrogen gas generated) over time in ambient air. (From ref. (12)).

The reported results on Al nanoparticles in Nafion membrane seem consistent with the same mechanistic picture proposed for Ag and Ag_2S nanoparticles. In the formation of these nanoparticles, the cavities and channels could apparently be rearranged (such as channels connecting two cavities being squeezed out for a larger cavity) to accommodate the growth of the nanoparticles toward their thermodynamically and/or kinetically preferred sizes, but still only up to a limit (likely 15 nm or less) imposed by the much more rigid perfluorinated polymer backbones in the membrane films (*15*, *24*, *25*). There were no dramatic increases in average particle sizes even at very high Al loadings. On the other hand, the high loadings of Al nanoparticles probably strained the membrane films so severely to make them vulnerable to decomposition (via grinding in a mortar, for example, as discussed above).

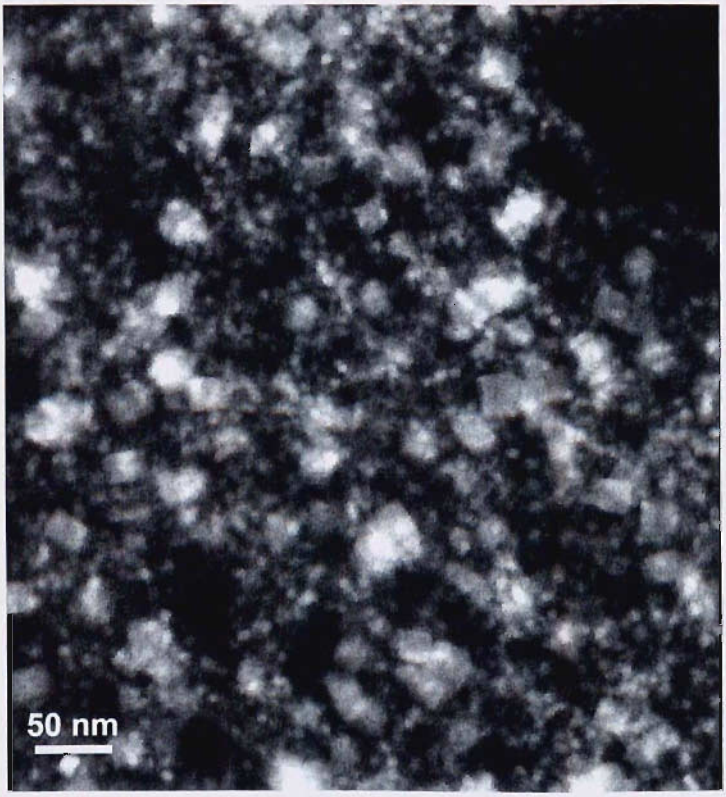

Figure 10. Representative scanning TEM image (in the Z-contrast mode) of the black-gray powdery Al-in-Nafion membrane with high Al loading (from grinding in a mortar and dispersing in hexane).

The nanocomposite-like configuration of nanoscale Al particles in perfluorinated ionomer membrane (Nafion) serves as an excellent platform for nano-energetic materials, similar to or more advantageous than those based on larger Al nanoparticles protected by fluorinated polymers (*10*, *11*). Separately, it also serves as an excellent platform for efficient hydrogen generation under ambient conditions. Further investigations may enable a regeneration of the Al nanoparticles in the nanoscale cavities of the membrane, so as to achieve rechargeable nano-Al systems for energy storage and hydrogen production.

4. Summary and Perspective

The results as examples presented and discussed here suggest that the structural cavities in perfluorinated ionomer membrane films serve as ideal nanoscale templates for facile preparation of well-dispersed small nanoparticles from semiconductors, metals, and other materials. For reactive nanoparticles, in particular, they are surprisingly intact and stable in the membrane films under ambient conditions, yet still accessible by other reactants (such as basic

water in the hydrogen generation) under a different set of conditions. The membrane films, which are macroscopically homogeneous and optically clean and transparent, also serve as excellent hosts for the nanoparticles to keep them dispersed. These spatially well-dispersed nanoparticles are unique photocatalysts for photochemically driven energy conversion applications. The membrane hosts are also valuable to another kind of energy conversion, potentially rechargeable reactive metal-based hydrogen production. However, despite the progress already made, the use of perfluorinated ionomer membranes in energy-related nanotechnology is still at the early stage. Further development and optimization are necessary, including a clear understanding of the structural details in the membrane films and the effects of the structure on transport properties of the membrane films (materials in and out of the nanoscale cavities in the membranes). Nevertheless, the nano-templating in these membrane films will find broad applications in energy conversion and beyond.

Acknowledgments

Financial support from the Air Force Research Laboratory through the nanoenergetics program is gratefully acknowledged. Additional supports from the South Carolina Space Grant Consortium (Y.-P.S.), the Air Force Office of Scientific Research (AFOSR) through the program of Dr. Julian Tishkoff (C.E.B.), the American Chemical Society Petroleum Research Fund (Y.-P.S.), the Cente for Advanced Engineering Fibers and Films at Clemson University (Y.-P.S.), and the Defense Threat Reduction Agency (DTRA) through the grant #HDTRA-07-1-0026 (E.A.G.) are also acknowledged.

References

1. (a) Kramer, K. W.; Biner, D.; Frei, G.; Gudel, H. U.; Hehlen, M. P.; Luthi, S. R. *Chem. Mater.* **2004**, *16*, 1244. (b) Shan, J. N.; Ju, Y. G. *Appl. Phys. Lett.* **2007**, *91*, 123103. (c) Shan, J. N.; Ju, Y. G. *Nanotechnology* **2009**, *20*, 275603.
2. Lorbeer, C.; Cybinska, J.; Mudring, A. V. *Chem. Commun.* **2010**, *46*, 571.
3. Gladysz, J. A., Curran, D. P., Horváth, I. T., Eds.; *Handbook of Fluorous Chemistry*; Wiley/VCH: Weinheim, Germany, 2004.
4. (a) Horvath, I. T.; Rabai, J. *Science* **1994**, *266*, 72. (b) Nyffeler, P. T.; Durn, S. G.; Burkart, M. D.; Vincent, S. P.; Wong, C.-H. *Angew. Chem. Int. Ed.* **2005**, *44*, 192. (c) Yang, C.; Wang, X. P.; Omary, M. A. *J. Am. Chem. Soc.* **2007**, *129*, 15454.
5. (a) Krishnan, M.; White, J. R.; Fox, M. A.; Bard, A. J. *J. Am. Chem. Soc.* **1983**, *105*, 7002. (b) Mau, A. W. H.; Huang, C. -B.; Kakuta, N.; Bard, A. J.; Campion, A.; Fox, M. A.; White, J. M.; Webber, S. E. *J. Am. Chem. Soc.* **1984**, *106*, 6537. (c) Kakuta, N.; White, J. M.; Campion, A.; Bard, A. J.; Fox, M. A.; Webber, S. E. *J. Phys. Chem.* **1985**, *89*, 48. (d) Kakuta, N.; Park, K. H.; Finlayson, M. F.; Ueno, A.; Bard, A. J.; Campion, A.; Fox, M. A.; Webber, S. E.; White, J. M. *J. Phys. Chem.* **1985**, *89*, 732. (e) Smotkin,

E. S.; Brown, R. M.; Radenburg, L. K.; Salomon, K.; Bard, A. J.; Campion, A.; Fox, M. A.; Mallouk, T. E.; Webber, S. E.; White, J. M. *J. Phys. Chem.* **1990**, *94*, 7543. (f) Zen, J.-M.; Chen, G. C.; Fan, F.-R. F.; Bard, A. J. *Chem. Phys. Lett.* **1990**, *169*, 23. (g) Li, F.; Bertoncello, P.; Ciani, I.; Mantovani, G.; Unwin, P. R. *Adv. Funct. Mater.* **2008**, *18*, 1685.

6. Premkumar, J.; Ramaraj, R. *J. Photochem. Photobiol. A* **1997**, *110*, 53.
7. Pathak, P.; Meziani, M. J.; Li, Y.; Cureton, L. T.; Sun, Y.-P. *Chem. Commun.* **2004**, 1234.
8. Pathak, P.; Meziani, M. J.; Castillo, L.; Sun, Y.-P. *Green Chem.* **2005**, *7*, 667.
9. (a) Lips, H. R. *J. Spacecraft Rockets* **1977**, *14*, 539. (b) Kubota, N.; Serizawa, C. *J. Propul. Power* **1987**, *3*, 303. (c) Watson, K. W.; Pantoya, M. L.; Levitas, V. I. *Comb. Flame* **2008**, *155*, 619.
10. (a) Jouet, R. J.; Warren, A. D.; Rosenberg, D. M.; Bellitto, V. J.; Park, K.; Zachariah, M. R. *Chem. Mater.* **2005**, *17*, 2987. (b) Jouet, R. J.; Carney, J. R.; Granholm, R. H.; Sandusky, H. W.; Warren, A. D. *Mater. Sci. Technol.* **2006**, *22*, 422.
11. Meziani, M. J.; Bunker, C. E.; Lu, F.; Li, H.; Wang, W.; Guliants, E. A.; Quinn, R. A.; Sun, Y.-P. *ACS Appl. Mater. Interfaces* **2009**, *1*, 703.
12. Li, H.; Meziani, M. J.; Lu, F.; Bunker, C. E.; Guliants, E. A.; Sun, Y.-P. *J. Phys. Chem. C* **2009**, *113*, 20539.
13. (a) Smart, B. E. *Organofluorine Chemistry – Principles and Commercial Applications*; Banks, R. E., Smart, B. E., Tatlow, J. C., Eds.; Plenum Press: New York, 1994, p 57. (b) Kissa, E. *Fluorinated Surfactants and Repellents*; Marcel Dekker, Inc.: New York, 2001. (c) Chambers, R. D. *Fluorine in Organic Chemistry*; Blackwell: Oxford, 2004. (d) Kirsch, P. *Modern Fluoroorganic Chemistry*; Wiley-VCH: Weinheim, Germany, 2004.
14. (a) Young, R. J. *Introduction to Polymers*; Chapman and Hall: New York, 1983, 204. (b) Kreuer, K. D., Paddison, S. J., Spohr, E.; Schuster, M. *Chem. Rev.* **2004**, *104*, 4637. (c) Smitha, B.; Sridhar, S.; Khan, A. A. *J. Membr. Sci.* **2005**, *259*, 10. (d) Cele, N.; Ray, S. S. *Macromol. Mater. Eng.* **2009**, *294*, 719.
15. Heitner-Wirguin, C. *J. Memb. Sci.* **1996**, *120*, 1.
16. Mauritz, K. A.; Moore, R. B. *Chem. Rev.* **2004**, *104*, 4535.
17. (a) Souzy, R.; Ameduri, B.; Boutevin, B.; Gebel, G.; Capron P. *Solid State Ionics* **2005**, *176*, 2839. (b) Gelbard, G. *Ind. Eng. Chem. Res.* **2005**, *44*, 8468.
18. (a) White, H. S.; Leddy, J.; Bard, A. J. *J. Am. Chem. Soc.* **1982**, *104*, 4811. (b) Buttry, D. A.; Saveant, J. M.; Anson, F. C. *J. Phys. Chem.* **1984**, *88*, 3086. (c) DiVirgilio-Thomas, M.; Heineman, W. R.; Seliskar, C. J. *Anal. Chem.* **2000**, *72*, 3461. (d) Bertoncello, P.; Ciani, I.; Li, F.; Unwin, P. R. *Langmuir* **2006**, *22*, 10380. (e) Bertoncello, P.; Ciani, I.; Marenduzzo, D.; Unwin, P. R. *J. Phys. Chem. C* **2007**, *111*, 294. (f) Bertoncello, P.; Dennany, L.; Forster, R. J.; Unwin, P. R. *Anal. Chem.* **2007**, *79*, 7549.
19. (a) Wang, S.; Lin, X. *Electrochim. Acta* **2005**, *50*, 2887. (b) Zhuo, Y.; Yuan, R.; Chai, Y.; Tang, D.; Zhang, Y.; Wang, N.; Li, X.; Zhu, Q. *Electrochem. Commun.* **2005**, *7*, 355. (c) Hrapovic, S.; Liu, Y.; Male, K. B.; Luong, J. H. T. *Anal. Chem.* **2004**, *76*, 1083. (d) Lim, S. H.; Wei, J.; Lin, J.; Li, Q.; You,

J. K. *Biosens. Bioelectron.* **2005**, *20*, 2341. (e) Bertoncello, P.; Peruffo, M.; Unwin, P. R. *Chem. Commun.* **2007**, 1597.
20. Rollins, H. W.; Lin, F.; Johnson, J.; Ma, J. J.; Liu, J. T.; Tu, M. H.; DesMarteau, D. D.; Sun, Y.-P. *Langmuir* **2000**, *21*, 8031.
21. Rollins, H. W.; Whiteside, T.; Shafer, G. J.; Ma, J. J.; Tu, M, H.; Liu, J. T.; DesMarteau, D. D.; Sun, Y.-P. *J. Mater. Chem.* **2000**, *10*, 2081.
22. Liu, P.; Bandara, J.; Lin, Y.; Elgin, D.; Allard, L. F.; Sun, Y.-P. *Langmuir* **2002**, *26*, 10398.
23. Sun, Y.-P.; Atorngitjawat, P.; Lin, Y.; Liu, P.; Pathak, P.; Bandara, J.; Elgin, D.; Zhang, M. Z. *J. Memb. Sci.* **2004**, *245*, 211.
24. Yeo, S. C.; Eisenberg, A. *J. Appl. Polym. Sci.* **1977**, *21*, 875.
25. Gierke, T. D.; Munn, G. E.; Wilson, F. C. *J. Polym. Sci.* **1981**, *19*, 1687. (c) Hsu, W. Y.; Gierke, T. D. *J. Membr. Sci.* **1983**, *13*, 307.
26. (a) Litt, M. H. *Polm. Prepr.* **1997**, *38*, 80. (b) Schmidt-Rohr, K.; Chen, Q. *Nat. Mater.* **2008**, *7*, 75.
27. (a) Bunker, C. E.; Ma, B.; Simmons, K. J.; Rollins, H. W.; Liu, J.-T.; Ma, J.-J.; Martin, C. W.; DesMarteau, D. D.; Sun, Y.-P. *J. Electroanal. Chem.* **1998**, *459*, 15. (b) Bunker, C. E.; Rollins, H. W.; Ma, B.; Simmons, K. J.; Liu, J.-T.; Ma, J.-J.; Martin, C. W.; DesMarteau, D. D.; Sun, Y.-P. *J. Photochem. Photobiol.* **1999**, *126*, 71.
28. (a) Lee, P. C.; Meisel, D. J. *J. Am. Chem. Soc.* **1980**, *102*, 5477. (b) Nagata, I.; Li, R.; Banks, E.; Okamoto, Y. *Macromolecules* **1983**, *16*, 903. (c) Kuczynski, J. P.; Milosavljevic, B. H.; Thomas, J. K. *J. Phys. Chem.* **1984**, *88*, 980. (d) Szentirmay, M. N.; Prieto, N. E.; Martin, C. R. *J. Phys. Chem.* **1985**, *89*, 3017. (e) Robertson, M. A.; Yeager, H. L. *Macromolecules* **1996**, *29*, 5166. (f) Anson, F. C.; Gray, H. B.; Sabatani, E.; Nikol, H. D. *J. Am. Chem. Soc.* **1996**, *118*, 1158.
29. (a) Fendler, J. H. *Nanoparticles and Nanostructured Films: Preparation, Characterisation and Applications*; Wiley-VCH: Weinheim, Germany, 1998. (b) Thomas, J. M.; Johnson, B. F. G.; Raja, R.; Sankar, G.; Midgley, P. A. *Acc. Chem. Res.* **2003**, *36*, 20.
30. (a) Haber, J. A.; Buhro, W. E. *J. Am. Chem. Soc.* **1998**, *120*, 10847. (b) Higa, K. T.; Johnson, C. E.; Hollins, R. A. U. S. Patent 5,885,321, 1999.
31. Foley, T. J.; Johnson, C. E.; Higa, K. T. *Chem. Mater.* **2005**, *17*, 4086.
32. Fernando, K. A. S.; Smith, M. J.; Harruf, B. A.; Lewis, W. K.; Guliants, E. A.; Bunker, C. E. *J. Phys. Chem. C* **2009**, *113*, 500.
33. Mahendiran, C.; Ganesan, R.; Gedanken, A. *Eur. J. Inorg. Chem.* **2009**, *14*, 2050.
34. (a) Mench, M. M.; Kuo, K. K.; Yeh, C. L.; Lu, Y. C. *Combust. Sci. Technol.* **1998**, *135*, 269. (b) Brousseau, P.; Anderson, C. J. *Propellants, Explos., Pyrotech.* **2002**, *27*, 300. (c) Granier, J. J.; Pantoya, M. L. *Combust. Flame* **2004**, *138*, 373.
35. (a) Roach, P. J.; Woodward, W. H.; Castleman, A. W., Jr.; Reber, A. C.; Khanna, S. N. *Science* **2009**, *323*, 492. (b) Wang, H.; Leung. D.; Leung, M.; Ni, M. *Renew. Sustain. Energ. Rev.* **2009**, *13*, 845.
36. (a) Weigle, J. C.; Luhrs, C. C.; Chen, C. K.; Perry, W. L.; Mang, J. T.; Nemer, M. B.; Lopez, G. P.; Phillips, J. *J. Phys. Chem. B* **2004**, *108*, 18601. (b)

Kwon, Y. S.; Gromov, A. A.; Strokova, J. I. *Appl. Surf. Sci.* **2007**, *253*, 5558.
37. Fedotova, T. D.; Glotov, O. G.; Zarko, V. E. *Propellants, Explos., Pyrotech.* **2000**, *25*, 325.